INSTITUTE OF INFORMATION AND COMMUNICATION TECHNOLOGIES
BULGARIAN ACADEMY OF SCIENCES
CYBERNETICS AND INFORMATION TECHNOLOGIES • Volume **26**, No 1
Sofia • 2026 Print ISSN: 1311-9702; Online ISSN: 1314-4081
DOI: 10.2478/cait-2026-0001

An Algorithm for Calculating Static Characteristics of Multi-Coordinate Electromagnetic Mechatronic Module

Isamiddin Siddikov[1], *Temurbek Rakhimov*[1], *Fazliddin Jumaniyazov*[2], *Guzal Khujaniyazova*[3], *Gulhayo Takhirova*[3]

[1]*Tashkent State Technical University named after Islam Karimov, Tashkent, Uzbekistan*
[2]*Mamun University, Khiva, Uzbekistan*
[3]*Urgench State University named after Abu Rayhon Beruni, Urgench, Uzbekistan*
E-mails: isamiddin54@gmail.com rahimov_timur@bk.ru zulfiqar-77@mail.ru guzalenka77@mail.ru gulhayo.taxirova@icloud.com

Abstract: *This paper presents an algorithm for calculating the static characteristics of a multi-coordinate electromagnetic mechatronic module. The proposed module features compact weight and dimensional parameters, enabling both linear and step movements in spatial coordinates with high accuracy and speed. A constructive calculation scheme is developed to investigate factors such as magnetic permeability along the conductivity coordinate under constant voltage supply, its rate of change, and the variation of electromagnetic force depending on the anchor displacement. For the holonomic module, which consists of electric, magnetic, and mechanical parts, the anchor is divided into non-magnetized sections to prevent flux branching in unexcited phases. The method employs a step-by-step approach for an inhomogeneous electromagnetic core, introducing a division of conductivity into central, external, and internal parts, which improves accuracy and efficiency. The developed mathematical models and algorithms allow the determination of boundary conditions, evaluation of elementary flux tubes, and validation through analytical and experimental comparison.*

Keywords: *Multi-coordinate electromagnetic mechatronic module, Static characteristics, Calculation algorithm, Constructive calculation scheme, Reciprocating movement.*

1. Introduction

When designing multi-coordinate electromagnetic mechatronic modules based on a linear electromagnetic motor, it is important to calculate their static characteristics in advance [1]. Methods based on solving magnetic field equations can be used to calculate the magnetic system and windings of multi-coordinate electromagnetic mechatronic modules, such as those based on linear electromagnetic motors, in various shapes. However, these methods are time-consuming in the calculation process, and the analysis of the results is complicated. Analytical methods are employed to calculate the electrical and magnetic components of multi-coordinate electromagnetic mechatronic modules, determine the conductance of magnetic flux paths, and assess the impact of various parameters on the attractive force. Also, these methods are effective, simple, and can be used by specialists in various fields in optimal calculation processes. These methods are effective for electromagnetic mechanisms and relays [2, 3], induction sensors, reciprocating motors [4], and stepper motors [5]. However, the existing analytical methods cannot be directly applied to multi-coordinate electromagnetic mechatronic modules based on linear electromagnetic motors, especially those with non-uniform anchor structures [6]. This is because this process is explained by the specific design features of linear electromagnetic motors [7, 8].

In related works, attention has also been paid to the improvement of control strategies under parameter variations [9] and the development of modular cyber-physical robotic systems with robust digital control to enhance operational flexibility and reduce technological cycle times [10].

For this reason, it is proposed to use the principle of superposition in the calculation of the gravitational force of the spherical electromagnetic core in the calculation of the static characteristics of the multi-coordinate electromagnetic mechatronic module [11]. In this method, a stepwise approach is applied to a single inhomogeneous electromagnetic core, where dividing the conductance between surfaces enhances both the efficiency and accuracy of the separation and calculation processes [12].

2. Research methodology

First, we consider the proposed design of the Multi-coordinate Electromagnetic Mechatronic Module (MEMM) [11]. The multi-coordinate electromagnetic mechatronic module design (Fig. 1) includes the following [1, 14, 15] parts: two symmetrical magnetic conductors 1, 2, and 3, a magnetic coil, a common anchor 4 made of ferromagnet, external pole parts with a conical ring 5, a rod 6, and an electromagnet firmly attached to it consists of 7 basic handle elements. The designations given in the design scheme of the multi-coordinate electromagnetic mechatronic module are: a – the current flow width; b – the length of the conical section of the anchor; c – the width of the stator pole section; d – the width of the stator pole section; e – the length of the cylindrical part of the anchor; α – the narrowed angle of current flow; β – the conical angle of the anchor. The values of α and β given here are used to calculate the structural parameters of the electromagnetic mechatronic module. The principle of operation of the structure is described as follows. When a control signal is given to the coil 3 and the electromagnetic base lever 7, the magnetic flux is induced, and the anchor 4 moves toward the stator pole 1, closing the magnetic circuit through its cylindrical and conical sections [16]. Under the influence of the electromagnetic force, the anchor tends to take a position corresponding to the minimum energy and moves to the right [2, 17]. Also, the grip element ensures the interaction of the executive body with the object in robotic systems. After that, the control signal is given to the reel 3, and the electromagnetic handle 7 is turned off, and by giving the control signal to the reel 2 and the electromagnetic handle 7, it ensures the return movement of the pole part of the anchor 1 to the side of the reel 3 and the return movement of the executive body [18].

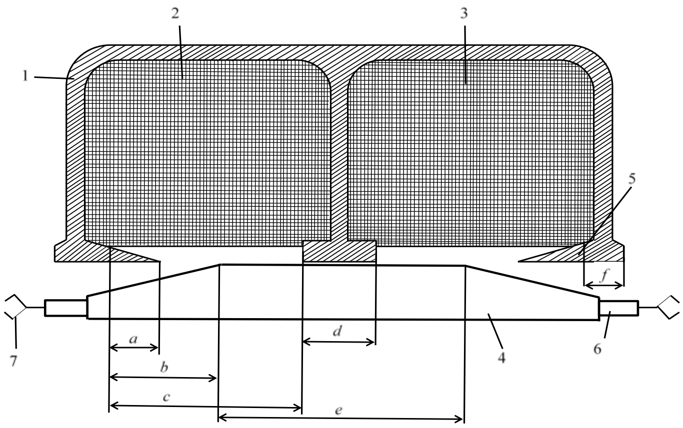

Fig. 1. Structural scheme of the multi-coordinate electromagnetic mechatronic module

Continuous operation of the anchor is maintained by modulating the conductance of the magnetic circuit within the mechatronic module. When the magnetic flux reaches its saturation point, the ring-shaped magnetic cone wave becomes saturated, causing a sharp reduction in its magnetic permeability [1, 14, 19]. The ring magnetic fluxes of the cone and their installation on the outer poles of the stator increase the performance of the holding element by increasing the traction characteristics at the end and beginning of the anchor step.

By calculating the static characteristics of the MEMM, it is possible to determine key parameters such as critical performance indicators, the boundary conductance between surfaces, and the spatial relationships among elementary flux tubes, the anchor, and the stator surfaces.

In reciprocating electromagnetic motors [16, 20], which are the basis of a multi-coordinate mechatronic module, the flux is evenly distributed along the magnetic circuit; therefore, in the critical area of the anchor movement, the electromagnetic force is generated by the interaction of magnetization through the flux. In cylindrical linear electromagnetic motors, which are the basis of MEMM, the structure of the electromagnetic core, the length of the coil corresponds to its thickness, and the pulling force in such a structure is mainly related to the pulling of the ferromagnetic element of the anchor, and the influence of the forces generated by the network currents on the poles of the exciting phase and its length is insignificant. Therefore, in devices with a heterogeneous structure [3, 21], the anchor is not separated by a magnet, the magnetic flux from the exciting phase is divided into adjacent (fixed) branches, and the interaction of the anchor with several poles is taken into account when calculating the pulling force.

In reciprocating electromagnetic motors, the movement of the anchor relative to the poles of the excited phase simultaneously causes a change in the magnetic [7, 11, 21] conductance in the two spaces between the surfaces of the ferromagnetic outer casing through the magnetic driving force (Fig. 2). The designations in the design calculation scheme of the multi-coordinate electromagnetic mechatronic module are as follows (Table 1).

Table 1. Used designations and their classifications

Designations	Classifications	Unit of measurement
A_1	Intermediate surface of 1-pole magnetic flux (surface area)	m^2
A_2	1 inner surface of the pole (surface area)	m^2
A_3	1 is the outer surface of the pole (surface area)	m^2
B_1	Intermediate surface of 2-pole magnetic flux (surface area)	m^2
B_2	Inner surface of 2 poles (surface area)	m^2
B_3	2 outer surface of the pole (surface area)	m^2
C_1, C_2, C_3, C_4	Anchor faces/sections	-
δ	The technical gap between the anchor and the stator	m
b	The distance between the poles	m
β	The angle between the surfaces	Radian (angle)
l	Is the effective length in the direction normal to the lines of force?	m
G	Magnetic Conductance between the anchor and stator surfaces	H (Henry)
r	The current radius of the arc of the circle of the elementary pipes	m
Φ	Magnetic flux	Wb
μ	Magnetic permeability	H/m
x_1 and x_2	Motion coordinates	m
R	Magnetic resistance	1/H
F_δ	Magnetic driving force	A (A·turn)
F_{EM}	Electromagnetic force	N

To calculate the static characteristics of the MEMM, the magnetic conductance (G) and its derivative are determined, followed by the electromagnetic force variation depending on displacement [1, 3, 22]. In addition, since in the considered multi-coordinate electromagnetic mechatronic module, the anchor is divided by non-magnetized connections, and the current from the excited phase does not branch to the neighboring non-excited ones, the calculation of the attraction force of the electromagnetic core is carried out by the superposition method [7, 10, 23].

Magnetic conduction lines can be calculated analytically using the method of circular arcs. Circular arcs form elementary tubes of magnetic conductance. The marginal conductivity between the corresponding surfaces is determined by generalizing the elementary tubes within the limits determined by the mutual location of the anchor and stator surfaces and some additional rational assumptions [14, 25]. Calculation of the static characteristics of the proposed multi-coordinate electromagnetic mechatronic module is performed step by step for one electromagnetic core. There are two methods of calculating the static characteristics of the electromagnetic mechatronic module: the first is the method based on dividing the anchor movement into a series of consecutive intervals [26], and the second is the method of calculating the characteristics through general mathematical expressions based on the simplification of the real process. Essentially, by employing the second calculation method, it is possible to determine the static characteristics of the MEMM and perform an initial estimation of the magnetic driving force. For this, the following stages of the sequence of calculating the static properties of MEMM can be formed:

At the 1st stage, for the parts of the anchor (C_1, C_2, C_3, C_4) of the multi-coordinate mechatronic module, a magnetic chain and taking into account the effective length of these parts according to l_1, l_2, l_3, l_4, according to the specified $x_1 > \delta$ conditions of the electromagnetic core, corresponding faces A_1 and C_1, determination of the magnetic [27] conductance between A_1 and C_1 is

(1) $$G(A_1C_1) = \int_{x_1}^{r_1+\delta+r_0} \frac{\mu_0 l dr}{\frac{\pi}{2r}} = \frac{2\mu_0\pi}{\pi} = \frac{r_1+\delta+r_0}{x_1},$$

where: r is the flow radius of the circular arc of elementary pipes passing from the surface of the anchor C_1 to the surface of the stator A_1; δ is the technical distance between the anchor and the stator; r_0 is the radius of the technological hole in the anchor; r_1 is the anchor radius; l is the effective length in the direction normal to the lines of force [28].

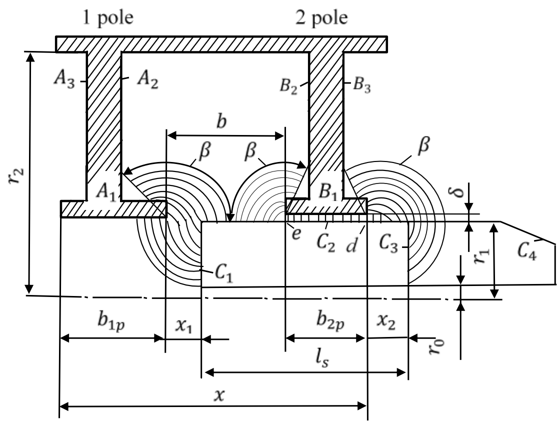

Fig. 2. Constructive calculation scheme of the multi-coordinate electromagnetic mechatronic module

The effective length can be calculated as the geometric distance between x_1 and $r_1 + \delta$, the radius of the average field line is equal to the radius of the circle minus $r_1 + \delta$ [1, 8, 29], it can be calculated as follows:

$$l = 2\pi\left[r_1 + \delta - \sqrt{x_1(r_1 + \delta)} \right].$$

Thus, the magnetic conductance between the faces A_1 and C_1 is determined by the expression

(2) $$G(A_1C_1) = 4\mu_0\left[r_1 + \delta - \sqrt{x_1(r_1 + \delta)}\right]\ln\frac{r_1+\delta-r_0}{x_1},$$

and conductance between faces A_2 and C_2 is

(3) $$G(A_2C_2) = 4\mu \int_{x_1}^{b/2} \frac{\mu_0 l dr}{\beta r} = \frac{\mu_0 l}{\beta} \ln \frac{b/2}{x_1},$$

where: *r* is the current radius of the arc of the circle of elementary pipes going from the surface A_2 to the surface C_2 of the anchor; μ is the magnetic permeability of the material; *b* is the distance between the surfaces of the fields; β is the angle between the surfaces [6, 26].

In this case, the effective length can be considered equal to $l = 2\pi\left[r_1 + \sqrt{\frac{x_1 b}{2}}\right]$.

Then, the magnetic conductance between the surfaces A_2 and C_2 [1, 3, 22] is

(4) $$G(A_2C_2) = \frac{2\pi\mu_0(r_1 + \sqrt{\frac{x_1 b}{2}}}{\beta} = \ln \frac{b/2}{x_1}.$$

To simplify the calculation, the conductance between surfaces A_2 and C_2 can be divided into three parts:

- conductance of the central part

(5) $$G(A_2C_1)_1 = 4.45\mu_0 \left(\frac{x_1 - \delta}{x_1}\right)\left(r_1 + \frac{\delta}{2}\right),$$

- conductance of the outer part

(6) $$G(A_2C_1)_2 = 9.92\mu_0 (r_1 + \frac{x_1}{2}),$$

- conductance of the interior

(7) $$G(A_2C_1)_3 = 0.92\mu_0 (r_1 + \delta - \frac{x_1}{2}).$$

In the interval $x_1 \le \delta$, the conductance between the corresponding faces of the pole [5, 29] is determined by the following formulas:

(8) $$G(A_2C_1) = \int_{\delta}^{r_1+\delta+r_0} \frac{\mu_0 l dr}{\frac{\pi}{2r}} = \frac{2\mu_0 l}{\pi} \ln\left(\frac{r_1+\delta+r_0}{\delta}\right),$$

$$l = 2\pi\left[r_1 + \sqrt{\delta(r_1+\delta)}\right],$$

(9) $$G(A_1C_1) = 4\mu_0\left[r_1 + \delta - \sqrt{\delta(r_1+\delta)}\right] \ln\left(\frac{r_1+\delta+r_0}{\delta}\right),$$

(10) $$G(A_2C_2) = \int_{\delta}^{b/2} \frac{\mu_0 l dr}{\beta r} = \frac{\mu_0 l}{\beta} \ln \frac{b/2}{\delta},$$

$$l = 2\pi(r + \sqrt{\delta(b/2)},$$

(11) $$G(A_2C_2) = \frac{2\pi\mu_0(r + \sqrt{\frac{\delta b}{2}})}{\beta} \ln \frac{b/2}{\delta},$$

(12) $$G(A_2C_1)_1 = 4.45\mu_0 (\frac{\delta - x_1}{\delta})(r_1 + \frac{\delta}{2}),$$

(13) $$G(A_2C_1)_1 = G(A_2C_1)_3 = 0.92\mu_0 (r_1 + \frac{\delta}{2}).$$

From the relations obtained for the condition of the first stage, we find the inductance created at the first pole of the stator:

$$G_1 = G(A_1C_1) + G(A_2C_2) + G(A_2C_1)_1 + G(A_2C_1)_2 + G(A_2C_1)_3.$$

According to the condition of the first stage, the terminal conductances at the pole of the second stator are determined as follows:

(14) $$G(B_2C_2) = \int_{\delta}^{b/2} \frac{\mu_0 ldr}{\beta r} = \frac{\mu_0 l}{\beta} \ln \frac{b/2}{\delta}.$$

The formula determines the effective length for this conductance. $l = 2\pi\left(r_1 + \sqrt{\frac{\delta b}{2}}\right)$, and taking into account it, the conductivity between faces B_2 and C_2 for this effective length is determined from the following expression:

(15) $$G(B_2C_2) = \frac{2\pi\mu_0\left(r_1 + \sqrt{\delta b/2}\right)}{\beta} \ln \frac{b/2}{\delta}.$$

The conductance between faces B_1 and C_2 is constant for this range:

(16) $$G(B_1C_2) = \frac{2\pi\mu_0\left(r_1 + \frac{\delta}{2}\right)b_{p2}}{\delta}.$$

The conductance between surfaces B_3 and C_2 is determined differently depending on the value of x_2.

If $x_2 \geq b/2$, the conductance between these surfaces is determined in the same way as the conductance between surfaces B_2 and C_2 (15).

If, $\delta < x_2 < b/2$; the anchor deviates to the left, the number of field lines passing from the B_3 surface to the C_2 surface decreases due to the formation of conductance, and it is observed that a part of the pipes passes from the B_3 surface to the C_3 surface with the formation [27] of conductance $G(B_3C_3)$. Therefore, we write the conductance $G(B_3C_2)$ in the form:

(17) $$G(B_3C_2) = \int_{\delta}^{x_2} \frac{\mu_0 ldr}{\beta r} = \frac{\mu_0 l}{\beta r} \ln \frac{x_2}{\delta}.$$

The effective length for this transmission is $l = 2\pi\left(r_1 + \sqrt{\delta x_2}\right)$, and in this case the transmission $G(B_3C_3)$ takes the following form:

(18) $$G(B_3C_2) = \frac{2\pi\mu_0\left(r_1 + \sqrt{\delta x_2}\right)}{\beta} \ln \frac{x_2}{\delta},$$

$G(B_3C_2)$ conduction is not observed for $x_2 < \delta$.

For $x_2 > b/2$; $G(B_3C_3)$ conductance is not observed, and in the interval $\delta \leq x_2 < b/2$ its deviation is observed when the anchor moves to the left:

(19) $$G(B_3C_3) = \int_{x_2}^{b/2} \frac{\mu_0 ldr}{\frac{\pi}{2r} + \beta(r + x_2)} = \frac{\mu_0 l}{\frac{\pi}{2r} + \beta} \ln \frac{\left(\frac{\pi}{2} + \beta\right)b + \beta x_2}{\left(\frac{\pi}{2} + \beta\right)x_2 + \beta x_2}.$$

The effective length can be taken as approximately $l = 2\pi r_1$. Then the calculation of conductance for $G(B_3C_3)$ takes the following form:

(20) $$G(B_3C_3) = \frac{2\pi r_1 \mu_0}{\frac{\pi}{2}+\beta} \ln \frac{\left(\frac{\pi}{2}+\beta\right)b + \beta x_2}{\left(\frac{\pi}{2}+\beta\right)x_2 + \beta x_2}.$$

If $x_2 \le \delta,$ the conductance $G(B_3C_3)$ is determined using the formula (19), and in this case δ is put instead of $x_2 \le \delta$.

In the case of concentric circles with the centers of the field lines at a point d and the radius of the largest concentric circle is equal to δ, the conductance G_d is constant and is determined by the following formula [28]:

(21) $$G_\mathrm{d} = 3.3\mu_0 \left(r_1 + \frac{\delta}{2}\right).$$

The conductance of G_e located at point e is determined in the same way:

(22) $$G_\mathrm{e} = 3.3\mu_0 \left(r_1 + \frac{\delta}{2}\right).$$

From the relations obtained for the conductance between the surfaces, the total conductance for the first range and pole 2 of the stator can be found as follows:

$$G_2 = G(B_2C_2) + G(B_1C_2) + G(B_3C_2) + G(B_3C_3) + C_\mathrm{d} + C_\mathrm{e}.$$

The synchronizing force is determined in the same way for other values of x, that is, the relationship $F_{\mathrm{EM}} = f(x)$ is formed.

As an example, we consider the calculation of electromagnetic forces acting on the anchor of a cylindrical-symmetric engine. The initial data for calculation are selected according to the structural parameters of the engine used to obtain static characteristics [1, 23, 25].

At the 2nd stage, the conductances G_1 and G_2 and their derivatives dG_1/dx and dG_2/dx for stator poles 1 and 2 are determined from the conductance of the parts separated from the results of the total conductance of the poles and stator for a given value of the x coordinate:

(23) $$\frac{dG_1}{dx} = \frac{dG(A_1C_1)}{dx} + \frac{dG(A_2C_2)}{dx} + \frac{dG(A_2C_1)_1}{dx} + \frac{dG(A2_2C_1)_2}{dx} + \\ + \frac{dG(A2_2C_1)_3}{dx},$$

(24) $$\frac{dG_2}{dx} = \frac{dG(B_3C_2)}{dx} + \frac{dG(B_3C_3)}{dx}.$$

The ElectroMagnetic Force $F_{\mathrm{EM}} = \frac{F_\delta^2}{2}$ is calculated depending on the movement of the anchor in the given constructive calculation scheme, where F_δ is the magnetic driving force, depending on the anchor moving in the space between the magnetic conductance and saturation dG_Σ/dx, and the conductance G_Σ – of the anchor-stator system is determined.

When the anchor is moved, the conductance changes in poles 1 and 2. Therefore, the product of the electromagnetic force and the conductance caused by the change in the magnetic driving force in the cavities is found by the sum of the electromagnetic forces generated in the poles 1 and 2:

(25) $$F_{\mathrm{EM}} = F_{\mathrm{EM1}} + F_{\mathrm{EM2}}.$$

Magnetic driving force in voids is calculated taking into account the magnetization curve of steel parts [3, 2, 28]. The magnetic circuit of the electromagnetic motor, which is the basis of the multi-coordinate mechatronic module, is divided into four parts: anchor, 1 pole, stator housing, 2 pole. Magnetic driving force is defined separately for individual parts of the magnetic circuit and air gaps. **The magnetic permeability μ of each steel part is considered in the calculation of magnetic resistance.**

It is also required to determine the resistance of the air gaps in poles 1 and 2, taking into account the magnetization curve of the magnetic driving force steel parts in the gaps.

In Step 3, the resistance of the air spaces in poles 1 and 2 $R_{\delta 1} = 1/G_1$ and $R_{\delta 2} = 1/G_2$ is determined;

The total electromagnetic force can be calculated by determining the magnetization curve of the magnetic driving force steel parts in the gaps and the resistance of the air gaps in poles 1 and 2:

(26) $$F_{\mathrm{EM}} = wl = H_1 l_1 + H_2 l_2 + H_3 l_3 + H_4 l_4 + \Phi(R_{\delta 1} + R_{\delta 1}),$$

where H_1, H_2, H_3, H_4 are the field strengths of the poles and the stator housing, and l_1, l_2, l_3, l_4 – the lengths of the anchor corresponding to it; w is the number of windings in the coil, and Φ is the current of the coil; $R_{\delta 1}$ and $R_{\delta 2}$ are the resistances of the air gap at the poles.

At the 4th stage, the magnetic flux is determined based on the relationship (7) according to the magnetic driving force given to the coil for individual parts of the magnetic circuit and air gaps. In this case, the calculation of the flow for the given magnetic driving force is carried out by the method of successive approximation. The first value of the magnetic flux $\Phi^{(1)}$ in pole 1 is determined without taking into account the magnetic resistance of the steel. Based on the known current value, $\Phi^{(1)}$ is determined in individual parts of the induction magnetic circuit, and based on the induction, using the magnetization curve of the electric steel [23-30], the voltages H_1, H_2, H_3, H_4 – on the surfaces A_1, A_2, A_3, B_1, B_2, B_3 – is determined the same for parts, and then magnetic driving force $F_{\mathrm{EM}}^{(1)}$ for 1 pole is determined using the expression (26). Also, by setting the new value of the current $\Phi^{(2)}$ in 2 poles, the magnetic driving force $F_{\mathrm{EM}}^{(2)}$ for 2 poles is determined. If the condition $\left|F_{\mathrm{EM}} - F_{\mathrm{EM}}^{(n)}\right| \leq \varepsilon$ is fulfilled, the iterative process ends, where the specified small value of F_{EM} with respect to error ε – is usually 0.5-1%. According to the found value of the magnetic flux, the magnetic driving force of the first and second pole gaps is determined:

(27) $$F_{\delta 1} = \Phi R_{\delta 1}, \ F_{\delta 2} = \Phi R_{\delta 2}.$$

In the 5th step, the magnetic driving force of spaces in poles 1 and 2 is determined based on the relation (27), where the force generated at poles 1 and 2 is determined by the following formulas, respectively:

(28) $$F_{\mathrm{EM1}} = \frac{F_{\delta 1}^2}{2}\frac{dG_1}{dx},$$

when the anchor of the MEMM moves to the left, it is negative, so the anchor movement is braked by the force created by the magnetic flux in the 2nd pole. The synchronizing force can be determined by taking into account the given value of the *x*-coordinate for the motion of the electromagnetic core and anchor of the 1 and 2 poles, and the magnetic driving force of the coil (25) and the forces generated in the 1 and 2 poles (28).

Determining the edge conductance of the matching boundary conditions for the deviation of the anchor from the average position for the case, $x_1 < \delta$ for the case $x_1 > \delta$ and for the case $x_2 \geq b/2$; the change of boundary conditions depending on the value of conductance x_2 between the surfaces B_3 and C_2, $\delta < x_2 < b/2$ then, the anchor deviation to the left represents the change of field lines passing from face B_3 to face C_2. The matching of these boundary conditions, the marginal conductance between the surfaces, the calculation of elementary tubes within the limits determined by the mutual location of the anchor and stator surfaces and some additional rational assumptions, and taking into account the comparison of experimental results and the development of an algorithm for calculating the static characteristics of a multi-coordinate electromagnetic mechatron module based on the presented mathematical models possible (Fig. 3). Based on the developed mathematical models, this algorithm calculates the structural static characteristics of the non-homogeneous multi-coordinate electromagnetic mechatronic module for one electromagnetic core in stages, and assumes the compliance of the entire multi-part structure with state changes and boundary conditions at the beginning and end of the working body.

In the main conditions of the calculation algorithm, the following is performed:

- in the first condition of the algorithm, the magnetic conductance poles of the stator are selected;
- in the second condition of the algorithm, the magnetic conductance is calculated for the initial position of the anchor for the selected poles or the space between the anchor and the stator;
- based on the determined results, the sum of the total conductance for each pole is calculated;
- based on the results of the conductance summation, conductances G_1 and G_2, and their derivatives dG_1/dx and dG_2/dx are determined for stator poles 1 and 2 for a given value of the *x*-coordinate of the anchor position;
- when the anchor moves, the electromagnetic force generated as a result of the change of the magnetic driving force in poles 1 and 2 is determined;
- the resistance of the air gaps in poles 1 and 2 is determined, taking into account the magnetization curve of the magnetic driving force steel parts in the gaps;
- calculating the current for a given magnetic driving force, the total electromagnetic force is calculated by determining the magnetization curve of steel parts and the resistance of the air spaces in poles 1 and 2 by the method of successive approximation;

- according to the found value of the magnetic flux, the magnetic driving force of the 1st and 2nd pole spaces is determined.

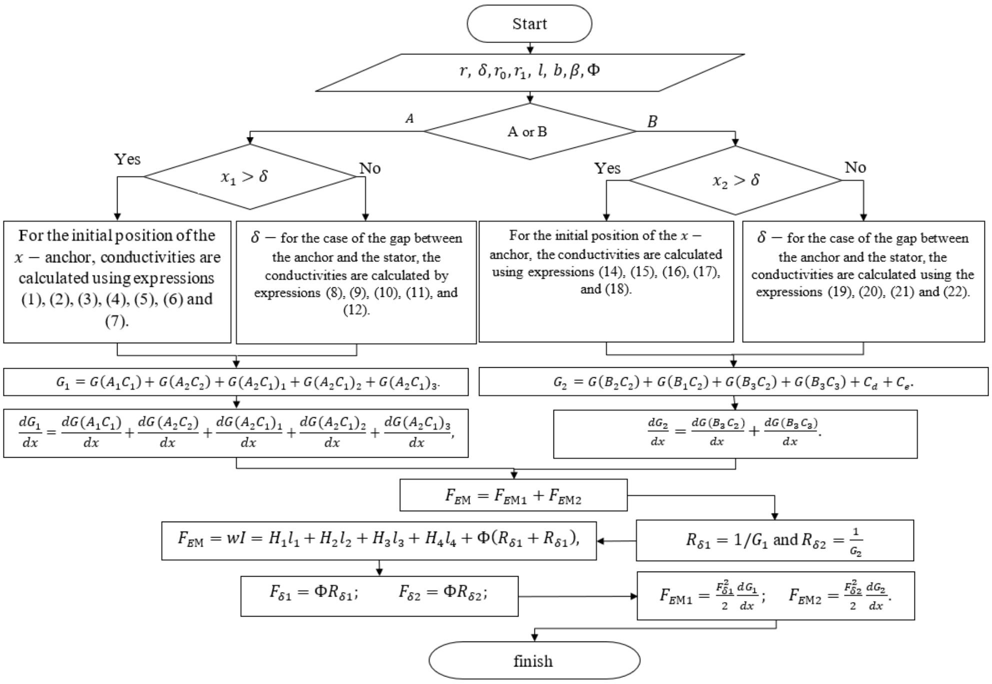

Fig. 3. Algorithm for the calculation of static characteristics of a multi-coordinate electromagnetic mechatronic module

On the basis of the mentioned formulas and equations, the initial data for calculating the static characteristics of the electromagnetic core of the linear electromagnetic motor, which is the basis of the multi-coordinate mechatronic module, l=0.06 m; r_2=0.07 m; r_3=0.075 m; b_{p1}=0.034 m; $\delta = 0.5 \times 10^{-5}$ m; b_{p2}=0.026; b=0.038 m; W=1290 wrap values are obtained. Calculate the effective length of the stator for a cylindrical anchor, l_s=0.066 m, and the radius size of the technological hole in the anchor r_1=0.02 m, and for a conical anchor l_{anch}=0.138 m; l_s=0.066 m; b_{p2}=0.026 m; It is done at values of $\theta_s = 0.32$ rad.

$X\times10^{-3}$m

In Fig. 4, for the cylindrical anchor, the continuous lines in green (1), red (2), and blue (3) represent the experimentally obtained static characteristics, while the black dashed lines correspond to the calculated results. The corresponding current values are 2 A, 4 A, and 3 A, respectively. In Fig. 5, for the conical anchor, the continuous lines in green (1) and purple (2) represent the experimentally obtained static characteristics, while the black dashed lines correspond to the calculated results. Here, the current values in the stator winding are 3 A and 4 A, respectively. From the characteristics of the static force curve, it should be noted that with large gaps $x_1 > b_{p1}$, the conductance of the main gap is small, and in the latter, the drop in magnetic driving force (almost equal to the magnetic driving force of the coil) is calculated almost depending on the anchor condition [1, 32, 33]. The characteristic of the conductance in this part of the anchor movement increases in the first gap, and in the second, it is almost zero, so the electromagnetic force increases. As the gap decreases, when the anchor is inserted into the pole gap, the conductance of the main gap increases, and its characteristic remains almost constant.

Comparison of the calculated and experimental results shows good qualitative agreement, with quantitative deviations within the engineering tolerance.

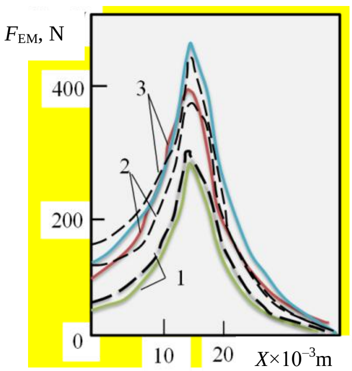

Fig. 4. Static characteristics of cylindrical anchor: Bold lines are experimentally obtained results.
Results of the calculation of ring lines

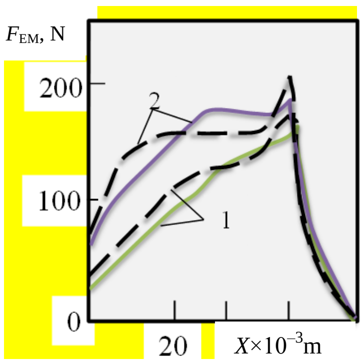

Fig. 5. Static characteristics of the conical anchor: bold lines are experimentally obtained results. Results of the calculation of ring lines

This, because the conductance of the main gap increases, and the magnetic driving force decreases when the anchor moves, which leads to a decrease in the constant $F_{\mathrm{EM}1}$ power. The transition from the increasing part to the decreasing part of the magnetic driving force forms a maximum, the abscissa of which lies in the area where these parts are separated.

3. Limitations

The MEMM belongs to systems operating based on electromagnetic actuators and can be used in the fields of mechatronics and robotics, in automatic control systems, as well as in mechanisms that provide linear-rotational motion of the actuator.

4. Conclusion

In the article, the construction of a multi-coordinate electromagnetic mechatronic module with high weight-gauge indicators, simplification of structural schemes, linear and step movements in space coordinates with high accuracy and speed, is proposed, and an algorithm for calculating its static characteristics is developed. The static characteristics of the device were analyzed depending on some factors, such as the magnetic **permeability** according to the conductance coordinate, its rate of change, and the change of the electromagnetic force depending on the anchor movement when the electromagnetic motor, which is the basis of the multi-coordinate mechatron module, is connected to a constant voltage. Based on these factors, a constructive calculation scheme of an electromagnetic mechatron module with a heterogeneous structure was developed, and it was proposed to use the principle of superposition in calculating the attraction force of an electromagnetic core due to the fact that the anchor is divided into non-magnetized parts and the magnetic flux is not branched into the non-excited ones in the excited phase. The calculation of the static characteristics of the multi-coordinate electromagnetic mechatronic module is carried out step by step for one inhomogeneous electromagnetic core, and it is proposed to divide the conduction between the surfaces into central, external, and internal parts, which serves to increase the efficiency of the calculation process. The developed algorithm calculates the external conductance between the surfaces, elemental tubes within the limits determined by the mutual location of the anchor and stator surfaces, and allows for comparing the experimental results, summarizing the analytical and experimental static results.

References

1. Glazunov, V. A. New Mechanisms in Modern Robotics. M., Tehnosfera, 2018. 316 p. (in Russian).
2. Jurevich, E. I. Fundamentals of Robotics. Second Ed. Peterburg, SPB PHV, 2005. 416 p. (in Russian).
3. Dang, A. T., M. Bosch-Mauchand, N. Arora, C. Prelle, J. Daaboul. Electromagnetic Modular Smart Surface Architecture and Control in a Microfactory Context. – Computers in Industry, Vol. **81**, September 2016, pp. 152-170.
4. Egorov, O. D., J. V. Poduraev. Design of Mechatronic Modules: Textbook. M., MGTU STANKIN, 2004. 360 p. (in Russian).
5. Angeles, J. Fundamentals of Robotic Mechanical Systems. Theory, Methods, Algorithms. Fourth Edition. New York, Springer, 2014.
6. Afonin, V. L. Processing Equipment Based on Parallel Structure Mechanisms. MGTU STANKIN, 2006. 452 p. (in Russian).
7. Afonin, A. A., R. R. Bilozor, V. V. Grebenikov, J. I. Dyhnenko, L. P. Mel'nichuk. Electromagnetic Drive of Robotic Systems. Kiev, Nauka, dumka, 1986. 272 p. (in Russian).
8. Nikitenko, A. G. Mathematical Modeling and Automation of Design of Traction Electric Vehicles. M., 1995. 610 p. (in Russian).
9. Karlova-Sergieva, V. Robust Performance Assessment of Control Systems with Root Contours Analysis. – Cybernetics and Information Technologies, Vol. **25**, 2025, No 2, pp. 83-99.
10. Guergov, S., N. G. Nikolova. Methodology for Designing Cyber-Physical Multi-Operation Robot Systems Operating in the Conditions of Digital Robust Control. – Cybernetics and Information Technologies, Vol. **23**, 2023, No 3, pp. 114-125.
11. Eleckaja, G. P., N. S. Ijulhina, A. P. Pankov. Electromechanical Systems. Tula, TulGU, 2009. 214 p. (in Russian).
12. Nazarov, K. N. Intelligent Multi-Coordinate Mechatronic Modules of Robotic Systems. Monografija, Toshkent, Mashhur-Press, 2019. 143 p. (in Russian).
13. Brodovskij, V. N., M. V. Baranov, J. V. Iljuhin. Mechatronic Drive Module for Translational Movement of Technological Machines. – Mehatronika, 2000, No 4 (in Russian).
14. Li, M. Developing a Portrait Drawing Robot with FANUC LR Mate 200id/4s. ICT Systems and Sustainability. – Singapore, Springer, 2022, pp. 491-497. DOI: 10.1007/978-981-16-5987-4_50.

15. B e d r i t s k i y, I. M., K. K. J u r a y e v a. Estimation of Errors in Calculations of Coils with Ferromagnetic Core. – In: Proc. of International Conference on Industrial Engineering, Applications and Manufacturing, ICIEAM'20, 2020, 9111943.
16. F a y z u l l a y e v, J. S., K. K. J u r a y e v a. The Transfer Function of a Traction Asynchronous Motor Controlled by a Four-Square Converter. – In: IOP Conference Series: Materials Science and Engineering, Vol. **734**, 2020, No 1, 012195
17. S i d d i k o v, I., T. R a k h i m o v. Parametric Optimization of a Multi-Output Electromagnetic Mechatron Module. – In: E3S Web of Conferences, 508, 2024, 01008. DOI: 10.1051/e3sconf/202450801008.
18. R a k h i m o v, T., U. M a t y o k u b o v, K. S o d i k o v. Algorithm for Controlling the Movement of an Intellectual Manipulator, Built Based on a Mechatron Module According to the Specified Trajectory and Position. – In: 26th IEEE International Conference of Young Professionals in Electron Devices and Materials (EDM'25), Altai, Russian Federation, 2025, pp. 2410-2415. DOI: 10.1109/EDM65517.2025.11096790.
19. M a t y o k u b o v, N. R., T. O. R a k h i m o v. Group Control of Functional Linear Actuation Elements of Mechatronic Modules. – Transactions of the Korean Institute of Electrical Engineers, Vol. **73**, 2024, No 6. DOI: 10.5370/KIEE.2024.73.6.995.
20. S u l t o n, A., T. K a m a l b e k, R. D i l s h o d. Experimental and Statistical Methods of Research and Optimization of Electric Power Systems Modes under Uncertainty Conditions Universum. – Technical Sciences, Vol. **107**, 2023, No 2-6, pp. 71-75.
21. D a v r o n b e k o v, D., M. M u r a d o v, D. M i r z a e v. Application Features of Supercapacitors in Energy Supply Systems. – In: Proc. of 8th International Conference on Future Networks & Distributed Systems (ICFNDS'24). Association for Computing Machinery, New York, NY, USA, 2025, pp. 314-318. DOI: 10.1145/3726122.3726168.
22. S i d d i k o v, I. K., T. O. R a k h i m o v, S. M. E r k i n o v. The Dynamics Calculating Algorithm of a Multi-Output Electromagnetic Mechatronic Module. – In: Proc. of 25th IEEE International Conference of Young Professionals in Electron Devices and Materials (EDM'24), Altai, Russian Federation, 2024, pp. 2570-2574. DOI: 10.1109/EDM61683.2024.10615168.
23. M a t y o k u b o v, N. R., T. O. R a k h i m o v. Structural-Mode Graphs of Electromagnetic and Mechatronic Modules of Intelligent Robots. – In: Proc. of 12th World Conference Intelligent System for Industrial Automation (WCIS'2022). DOI: 10.1007/978-3-031-53488-1_30.
24. I l j u h i n a, N. S., A. A. F r o l o v, L. V. B e l e c k a j a. Study of Static and Dynamic Characteristics of Electromagnetic Steering Drives. Izvestija TulGTU. Tehnicheskie nauki, 2011. Vyp. 5. Ch. 1 (in Russian).
25. N a z a r o v, K. N., N. R. M a t y o k u b o v, T. O. R a k h i m o v. Algorithm for Calculating the Parameters of a Multi-Position Electromagnetic Linear Mechatronic Module. – Chemical Technology, Control and Management, Vol. **2021**, 2021, Issue 6, Article 7. DOI: 10.51346/tstu-02.21.6-77-0051.
26. M a t y o k u b o v, U. K., M. M. M u r a d o v, J. F. Y u l d o s h e v. Development of the Method and Algorithm of Supplying the Mobile Communication Base Station with Uninterrupted Electrical Energy. – In: Proc. of 25th IEEE International Conference of Young Professionals in Electron Devices and Materials (EDM'24), Altai, Russian Federation, 2024, pp. 2400-2406. DOI: 10.1109/EDM61683.2024.10615043.
27. A r h i p o v a, E. V., N. V. R u s s o v a, G. P. S v i n c o v. Improved Method of Design Calculation of DC Armoured Electromagnets with Insertion Anchors. – Vestnik Chuvashskogo Universiteta, 2013, No 3, pp. 156-161 (in Russian).
28. A f o n i n, A. A., V. V. G r e b e n n i k o v. Linear Electromagnetic Drive and Calculation of Its Static and Dynamic Characteristics. – Kiev, Preprint, 1981. 55 p.
29. G o s i e w s k i, Z., K. F a l k o w s k i, M. Z o k o w s k i. Introductory Analysis of the Bearingless Induction Motor. – Solid State Phenomena, Vol. **147**, 2009, No 149, pp. 143-148. Main Theme: Mechatronic Systems and Materials III. DOI: 10.4028/www.scientific.net/SSP.147-149.143.
30. G o s i e w s k i, Z., M. K o n d r a t i u k. Selection of Coil Parameters in Magnetic Launchers. – Solid State Phenomena, Vol. **147-149**, 2009, pp. 438-443. Main Theme: Mechatronic Systems and Materials III. DOI: 10.4028/www.scientific.net/SSP.147-149.438.

31. J u s t, K., P. P i s k u r. Static Analysis of the Tubular Electromagnetic Linearactuator with Permanent Magnets. – Scientific Journal of Polish Naval Academy (Zeszyty Naukowe We Akademii Marynarki Wojennej), 2018 (LIX) 2 (213). DOI: 10.2478/sjpna-2018-0015.
32. R i s t i c-D j u r o v i c, J. L., S. S. G a j i c, A. Z. I l i c et al. Design and Optimization of Electromagnets for Biomedical Experiments with Static Magnetic and ELF Electromagnetic Fields. – IEEE Transactions on Industrial Electronics, Vol. **65**, 2018, Issue 6, pp. 4991-5000.
33. M a t y o k u b o v, U. K., M. M. M u r a d o v. Comparison of Routing Methods in Wireless Sensor Networks. – In: Proc. of 16th IEEE International Scientific and Technical Conference Actual Problems of Electronic Instrument Engineering (APEIE'23), Novosibirsk, Russian Federation, 2023, pp. 1780-1784. DOI: 10.1109/APEIE59731.2023.10347799.

Received: 25.09.2025, First revision: 21.10.2025, Second revision: 10.11.2025, Accepted: 15.11.2025